Electronic Supplementary Material (ESI) for Nanoscale.

SUPPORTING INFORMATION

Biodegradable zwitterionic nanoparticles with tunable UCST-type phase separation under physiological conditions

Mattia Sponchioni[1,2], Paola Rodrigues Bassam[2], Davide Moscatelli[2], Paolo Arosio[1], and, Umberto Capasso Palmiero[1,]*

[1]Department of Chemistry and Applied Biosciences, Institute for Chemical and Bioengineering, ETH Zurich, Vladimir-Prelog-Weg 1, 8093 Zurich, Switzerland.
[2]Department of Chemistry, Materials and Chemical Engineering "Giulio Natta", Politecnico di Milano, Via Mancinelli 7, 20131 Milano, Italy.
* Corresponding author: Umberto Capasso Palmiero; E-mail: umberto.capasso@chem.ethz.ch

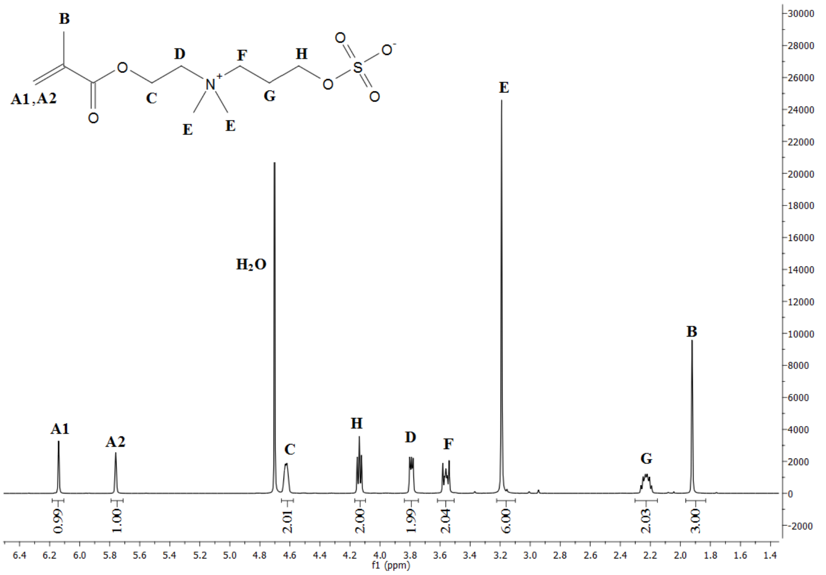

Figure S1. ^{1}**H NMR spectrum of the sulfabetaine methacrylate (ZB). The spectrum was recorded on a Bruker 400 MHz spectrometer using deuterium oxide as solvent.**

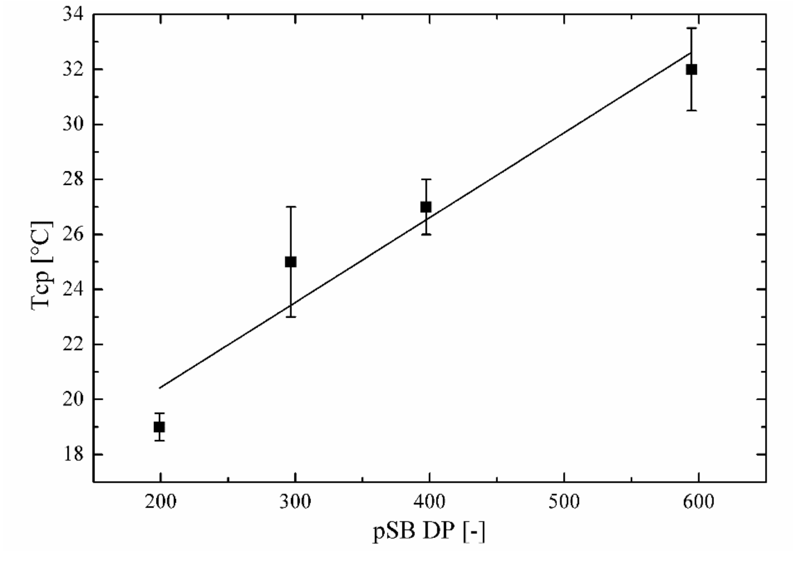

Figure S2. Influence of the pSB degree of polymerization (DP) over the polymer cloud point (Tcp), evaluated for 5% w/w polymer solutions in pure water.

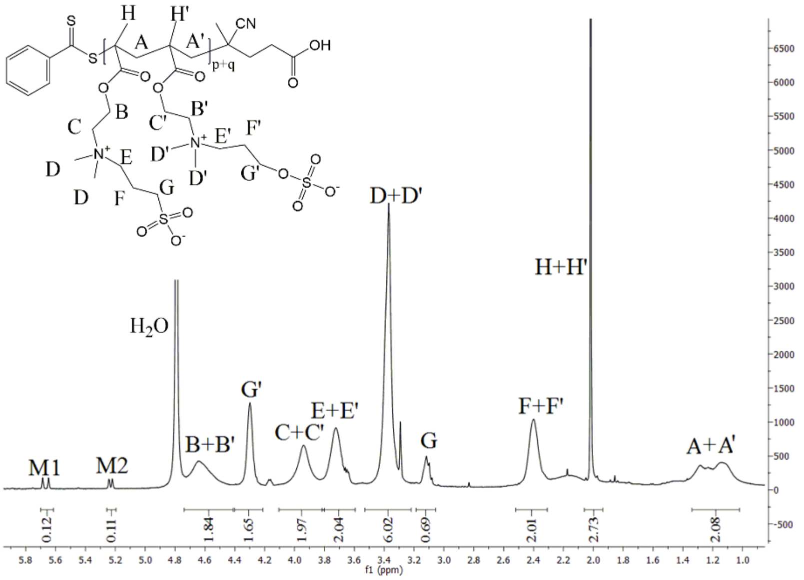

Figure S3. ^{1}H NMR spectrum of the p(60SB-140ZB), reported as an example. The spectrum was recorded on a Bruker 400 MHz spectrometer using deuterium oxide as solvent. Peaks M1 and M2 refer to the vinyl hydrogens of the unreacted monomers, not shown in the figure.

The monomer conversion (χ) can be calculated from the ^{1}H NMR spectra of the p(SB-*co*-ZB) copolymers according to Equation S1, where the letters refer to the peak labelling reported in **Figure S3** referred to the p(60SB-140ZB), as an example.

$$\chi = 1 - \frac{6M1}{D + D'} \tag{S1}$$

From the ^{1}H NMR spectra, it is also possible to evaluate the ZB mole fraction in the statistical copolymer (r_{ZB}) according to Equation S2.

$$r_{ZB} = \frac{G'}{G + G'} \tag{S2}$$

The values of r_{ZB} are summarized, for the different copolymers, in **Table S1**.

Table S1. Number average molecular weight (Mn), polydispersity (*Đ*), monomer conversion (χ), ZB mole fraction in the copolymer (r_{ZB}) and Tcp measured for the pSB and p(SB-*co*-ZB) polymers. The latter parameter was measured in both water and physiological solution at a polymer concentration of 5 % w/w.

Sample	Mn (Da)[a]	*Đ* (-)[a]	χ^b (-)	$r_{ZB}{}^b$ (-)	Tcp H_2O (°C)	Tcp 0.9% NaCl (°C)
200SB	21500	1.23	0.94	0	19	≤ 4
300SB	26800	1.21	0.97	0	25	≤ 4
400SB	33100	1.22	0.94	0	27	≤ 4
600SB	44300	1.30	0.91	0	32	≤ 4
0SB-200ZB	9700	1.19	0.99	1	≥ 100	≥ 100
50SB-150ZB	18400	1.14	0.89	0.78	≥ 100	70-75
60SB-140ZB	17400	1.19	0.91	0.70	≥ 100	34
70SB-130ZB	16400	1.21	0.92	0.66	≥ 100	31
80SB-120ZB	17000	1.22	0.90	0.63	90-95	29
90SB-110ZB	21900	1.15	0.95	0.54	75-80	25
100SB-100ZB	20500	1.18	0.91	0.48	75-80	22
110SB-90ZB	16800	1.19	0.97	0.43	37	≤ 4
120SB-80ZB	17800	1.20	0.93	0.39	32	≤ 4
130SB-70ZB	19200	1.18	0.92	0.33	22	≤ 4
140SB-60ZB	20000	1.19	0.88	0.28	26	≤ 4
150SB-50ZB	21700	1.21	0.90	0.22	23	≤ 4
200SB-0ZB	20900	1.21	0.94	0	19	≤ 4

[a] Measured from GPC

[b] Measured from ^{1}H NMR

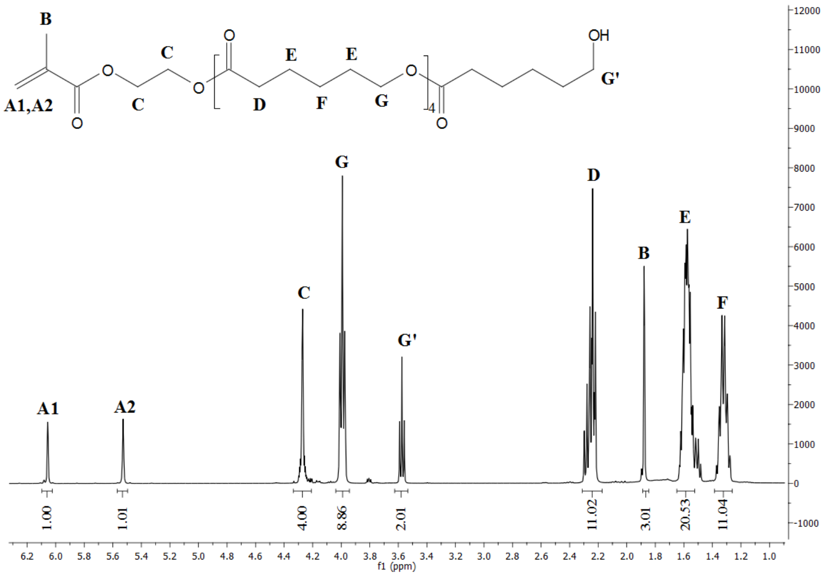

Figure S4. ^{1}H NMR spectrum of the HEMACL$_5$ macromonomer synthesized via the ROP of CL initiated by HEMA. The spectrum was recorded on a Bruker 400 MHz spectrometer using deuterated chloroform as solvent.

The mean degree of polymerization (DP) for the macromonomers produced via ROP (i.e. HEMACL$_n$) was evaluated by comparing the integral of peaks G and G' (according to the labelling of **Figure S4**), following Equation S3.

$$DP = \frac{G}{G'} + 1 \tag{S3}$$

In the specific case of the HEMACL$_5$, whose spectrum is reported in **Figure S4**, the mean is equal to 5.4, which is very close to the target. With similar considerations, the CL conversion (χ) and DP and the macromonomer molecular weight are reported in **Table S2** for the four synthesized macromonomers.

Table S2. Properties of the different macromonomers produced via ROP by changing the ratio [CL]/[HEMA].

Sample	χ_{CL}	DP	MW (Da)	MW$_{theoretical}$ (Da)
HEMACL	0.92	1.1	255.69	244.28
HEMACL$_3$	0.98	3.3	505.09	472.56
HEMACL$_5$	0.98	5.4	736.00	700.84

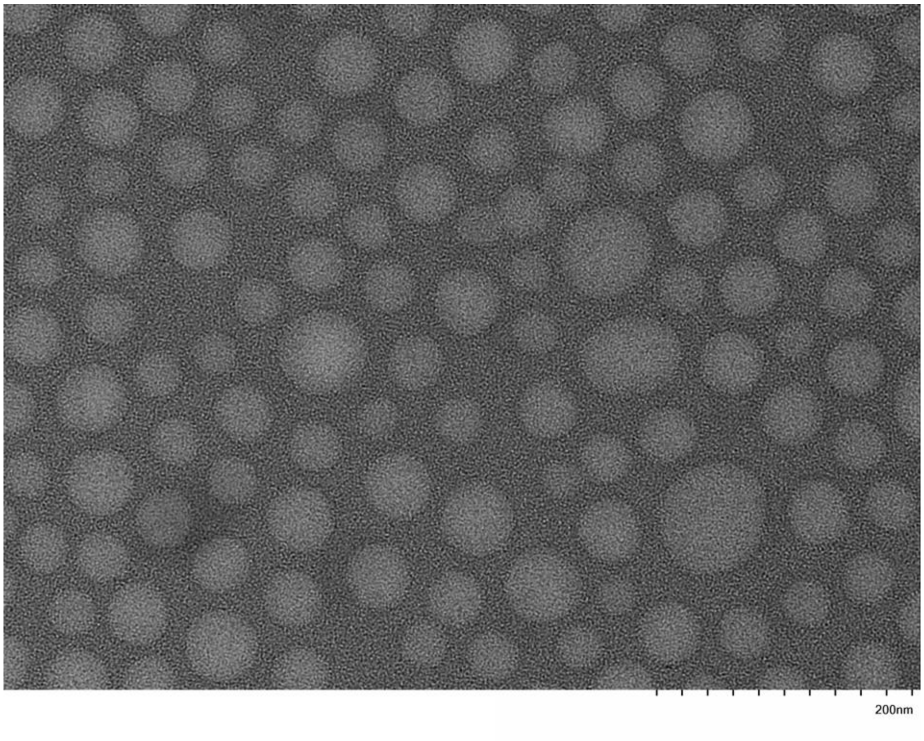

Figure S5. TEM image of the zwitterionic nanoparticles composed of p(110SB-90ZB)-*b*-(20HEMACL$_3$) block copolymers. The zwitterionic nanoparticles have a spherical morphology.

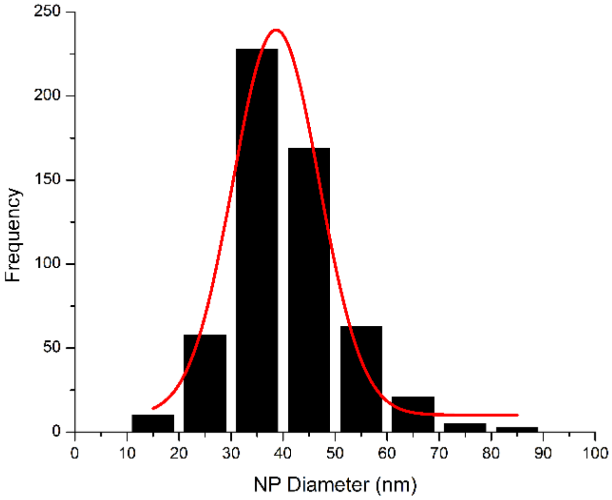

Figure S6. NP size distribution of the zwitterionic nanoparticles composed of p(110SB-90ZB)-*b*-(20HEMACL$_3$) block copolymers reconstructed from 6 different TEM images. Image processing and data analysis were performed on ImageJ and Origin 8, respectively. Average NP Diameter = 39 nm. Polydispersity = 21 %. The zwitterionic nanoparticles have a relatively narrow particle size distribution. The average NP diameter obtained via TEM is smaller compared to the corresponding average hydrodynamic diameter obtained via DLS. This phenomenon is ascribed to the absence of the hydration layer in the TEM analysis (the nanoparticles are dried before analysis) and to the bias of light scattering techniques (e.g. DLS) towards bigger nanoparticles.

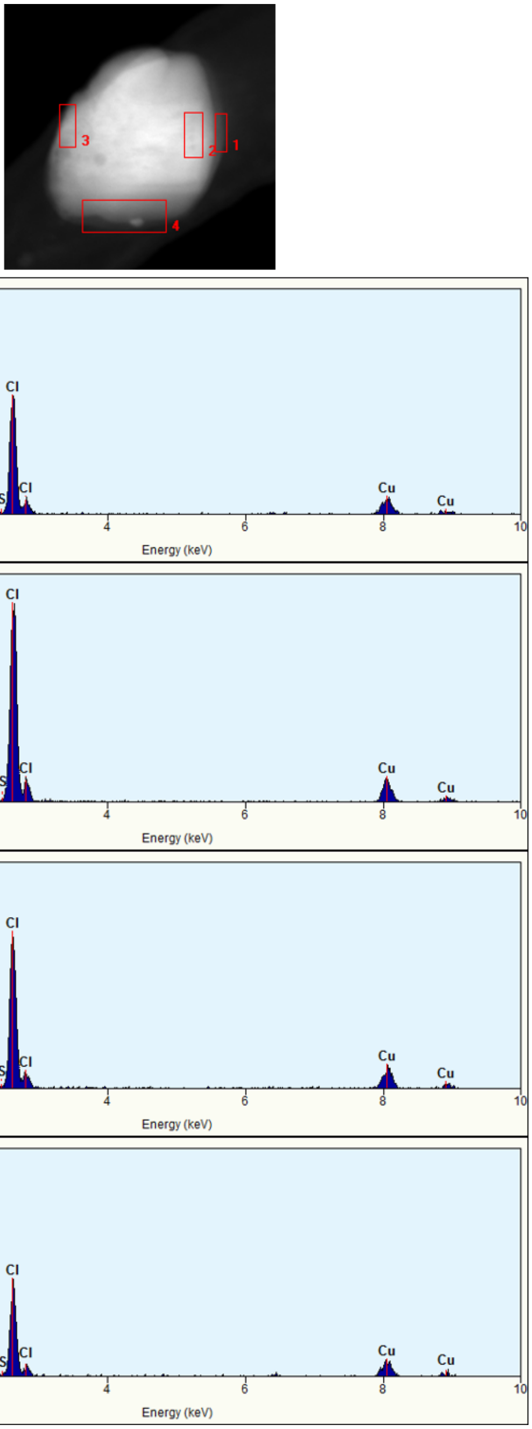

Figure S7. Elemental analysis via EDXS of different zones (1-4) of a single zwitterionic nanoparticle composed of p(110SB-90ZB)-*b*-(20HEMACL$_3$) block copolymers. The elemental analysis of particle`s rim areas show increase sulfur (S) content compared to the core. The preferential confinement of the sulfate bearing zwitterionic portion of the block copolymers on the NP surface hints to a NP core-shell structure.

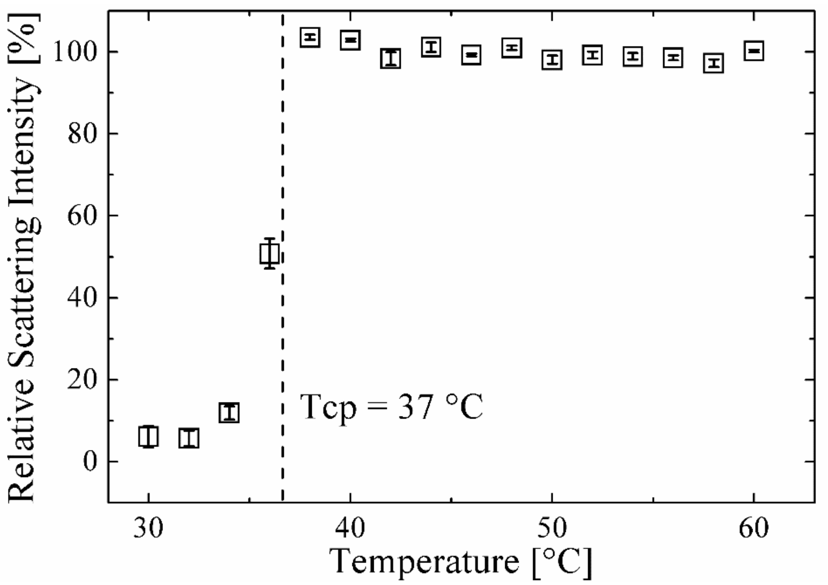

Figure S8. Scattering intensity at increasing temperature for the sample p(110SB-90ZB)-*b*-(20HEMACL$_3$) at 5% w/w in physiological solution. The sample was incubated at 30 °C for 30 minutes before starting the measurement. The temperature was raised by 2 °C for each measurement and the sample equilibrated for 10 minutes before the analysis. The Tcp was evaluated as the inflection point of the relative scattering intensity curve.

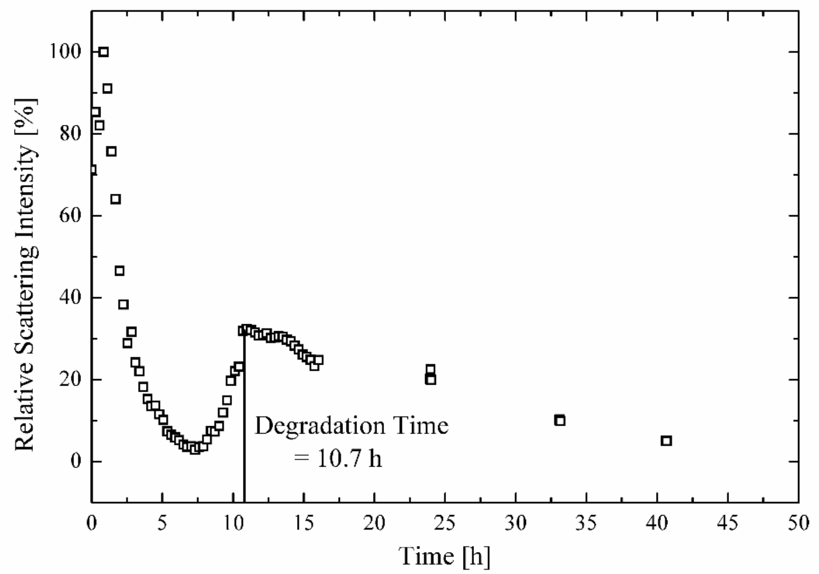

Figure S9. Relative scattering intensity measured at the DLS for the microaggregates obtained from p(110SB-90ZB)-*b*-p(20HEMACL$_3$). The measurement was performed at 37 °C under accelerated degradation conditions (pH = 14) and monitoring the scattering intensity during time. The degradation time was considered as the time corresponding to the secondary maximum of the curve. This point is associated to the release of primary particles from the microaggregates due to the decrease in the Tcp below the measurement temperature, as a result of the reduction in the length of the lateral oligoester chains following hydrolysis.

Table S3. Ratio between the intensities of the third band (384 nm, I_3) to the first band (373 nm, I_1) of the pyrene emission spectra at different temperatures for polymer NPs at 1% w/w.

Sample	Temperature (°C)	I_3/I_1
p(110SB-90ZB)-*b*-p(20HEMACL$_3$)	30	0.609±0.007
	45	0.590±0.003

The I_3/I_1 ratios reported in **Table S3** at two values of temperature are obtained from the pyrene emission spectra shown in **Figure S10**.

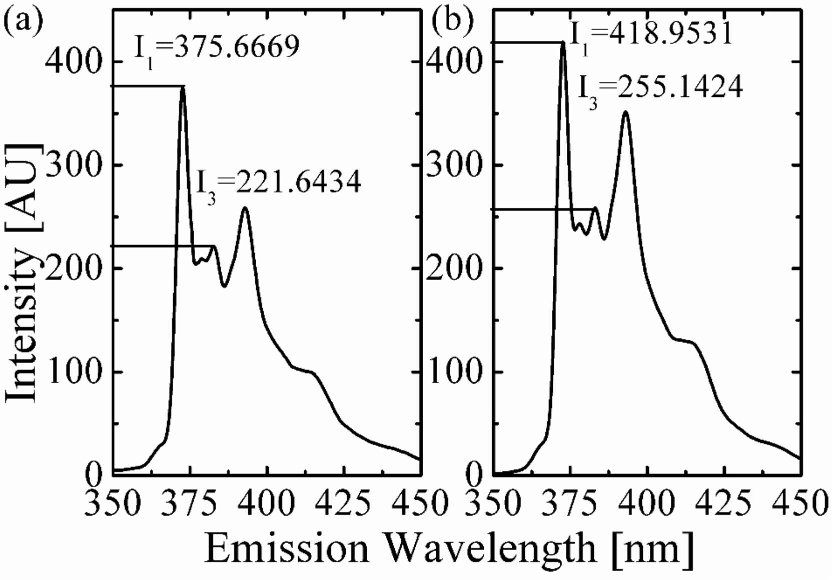

Figure S10. Pyrene emission spectra recorded after incubation for 24 h with p(110SB-90ZB)-*b*-(20HEMACL3) NPs (5% w/w) at: a) 30 °C) and b) 45 °C. The excitation wavelength is in both cases 335 nm. The different polarities of the environment where pyrene is located is also confirmed by the different resolution between the second (378 nm) and the third peak (384 nm). In particular, the resolution is enhanced when pyrene is in the lipophilic microenvironment of the NP core.

Movie S1. Phase separation tracked at the epi-fluorescence microscope (Eclipse Ti-E, Nikon) equipped with an Omicron LedHub Light engine. The data acquisition was obtained using a 384-well plate (MatriPlate, Glass Bottom, Brooks). The sample p(60SB-140ZB) was dissolved in PBS with a concentration of 5% w/w at room temperature. The solution was incubated at 45 °C and then analyzed at the microscope with a 60x objective at progressively decreasing temperature. The formation of polymer-rich liquid droplets that coalesce leading to a continuous liquid phase can be observed once the temperature is reduced below the Tcp of the copolymer (i.e. 35 °C).

Movie S2. Phase separation of the p(110SB-90ZB)-*b*-p(20HEMACL$_3$) based NPs tracked with the epi-fluorescence microscope (Eclipse Ti-E, Nikon). The NP dispersion at 5% w/w in PBS was heated to 45 °C and then observed at the microscope with a 60x objective at decreasing temperature. The formation of microaggregates can be observed below the Tcp (i.e. 37 °C).